3-11

THE BEHAVIOR OF RC BEAMS WITH CFRP BARS ANALYZED BY USING FINITE ELEMENT METHOD

Industrial Technology of Nihon University	○ Ming-Chien HSU
National Taipei University of Technology	Yeou-Fong LI
Industrial Technology of Nihon University	Tetukazu KIDA; Tadashi ABE
	Toshiaki SAWANO

1. Introduction

Over the years, reinforced concrete (RC) structures were damaged by the natural weather, earthquakes, and overloading. The most critical effects to the RC structures are chloride contamination and corrosion of rebars, which mostly affect the steel rebars in the RC structures. Therefore, finding a substitute material for the steel rebars is one of the focuses of researchers. The fiber reinforced plastic (FRP) [1, 2, 3] composite material has been considered as one of the best materials substitute to steel rebar since it has anti-corrosion, lightweight, as well as high strength and high elastic modulus properties. In this paper, the authors used carbon fiber reinforced plastic (CFRP) bars as the reinforcement at the tensile side of the RC beams [4, 5, 6] instead of steel rebars. By understanding the behavior of CFRP bars in RC beams, the maximum flexural strength of the RC beam and the strength of CFRP bars will be considered. Moreover, RC beams were calculated by using finite element method (FEM) in this paper.

2. Preparation of Experimental Specimens

2.1 Materials used for experimental specimens

Normal concrete with the compression strength of 22.45 N/mm^2 was used for the RC beams in the experiments. This uniaxial concrete compression strength was obtained from the laboratory, and the young's modulus was found form it. The CFRP bars, similar in size to D10 steel rebars, were used in the tensile side of the RC beams. D16 was used in the compression side of the RC beams and D10 was used as the steel stirrup. The properties of concrete, steel rebars and CFRP bars are shown in Table 1 and Table 2 [4, 5, 6].

2.2 Specimen size and steel rebar arrangement

All the RC beam's specimens were 180×220×1350 mm in size. However, the arrangements of tensile reinforcements were different. There were three different arrangements of the rebars in the tensile side of the RC beams for experiments. In the first type, the CFRP bars were placed at the center of the RC beam located at the tensile side and two D16 Steel rebars located at the compression side. The D10 steel stirrups were included in the RC beams with a distance of 80 mm between each other. However, the steel stirrups were not placed within a 300 mm range at the center of the RC beams. For the second type, there are two D10 CFRP bars placed at the tensile side with the center-to-center distance of 104 mm away from each others. Other steel rebar setups were same as Type One for the compression side and the steel stirrups. For the third type, there are three D10 CFRP bars placed at the tensile side with the center-to-center distance of 52 mm away from each others. Other steel rebars setups were the same as Type One for the compression side and the steel stirrups.

Fig. 1 shows one example of the RC beam with one CFRP bar in the tensile side, the dimensions, and other layouts for the experiment. Hereafter, the RC beams with one, two and three longitudinal CFRP bars are named N-C1S2, N-C2S2, and N-C3S2, respectively. The N indicates the normal strength concrete. The C indicates the CFRP bars. The numbers indicate the number of rebars located at the tensile side and the

Table 1 Concrete and steel rebar material properties

Test specimen	Concrete		Steel rebar (SD295A / D16)		
	Compressive strength (N/mm^2)	Young's modulus (N/mm^2)	Yield strength (N/mm^2)	Tensile strength (N/mm^2)	Young's modulus (kN/mm^2)
N-CS	22.45	5600	395.71	520	200

Table 2 CFRP bar's material properties

Name of CFRP	Cross Section (mm^2)	Tensile strength (N/mm^2)	Young's modulus (kN/mm^2)
CFRP bars	72.48	854.72	92.12

有限要素方法による CFRP 筋使用 RC 梁挙動解析

徐　銘謙、李有豊、木田哲量、阿部　忠、澤野利章

compression side.

2.3 Experimental method

The monotonic loading was carried out, and the loading area was 180×300 mm at the center of the span. The load was increased until the experimental specimens failed. The deflections of the RC beams were being recorded during the experiments. Fig. 1 shows the location of the loading area.

3. FEM Analysis of RC Beams

The three-dimensional RC beam's finite element model was created by DIANA [7] to simulate the specimens under monotonic loading. Moreover, an eight-node iso-parametric solid brick element was used for the concrete elements. The longitudinal steel rebars, CFRP bars and steel stirrups were included in the model, as well. However, the authors assume the interface between steel rebars and concrete was fully bonding. Also, it was the same as the interface between the CFRP bars and the concrete.

3.1 Constitutive parameter

The material properties for the concrete, the steel rebars and CFRP bars were obtained from the laboratory tests. However, some material properties of the concrete and steel were adopted from the specification for concrete structures in Japan [8], such as concrete tensile strength, concrete tensile ultimate strain, concrete compression yield strength, steel rebar after yielding, and etc.

(1) Concrete tensile strength

The tensile strength was calculated from the compressive strength and shown in Fig. 2 (a) that was from the Standard Specifications for Concrete Structures. [8] For the concrete tensile softening curve, the linear tensile softening was chosen from DIANA's manual [7]. The ultimate tensile strain in the softening curve is shown in Fig. 2 (a). The shear retention should also consider into the cracking modeling, and the full shear retention was used in the modeling of concrete cracking. On the other hand, the shear modulus did not reduce in the calculation. For the concrete cracking, the Smeared-cracking modeling [7,9,10] would be used.

(2) Concrete compressive strength

The uniaxial compressive test of concrete had been done in the laboratory. The compressive strengths are listed in Table 1 and the relevant strain of maximum compressive strength was 0.006 [4,5,6]. However, the characteristic of the compressive curve needs to be adopted from the Standard Specifications for Concrete
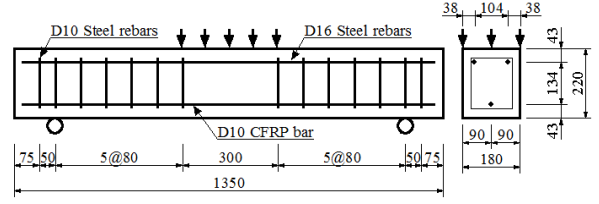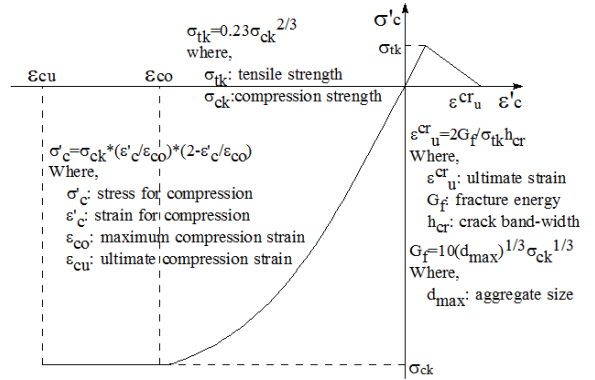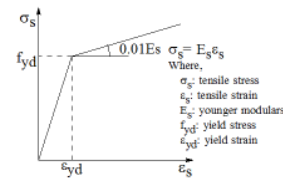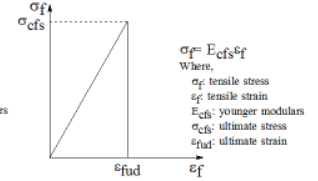

Fig. 1 The dimension and rebars arrangement of RC beams (For example: N-C1S2) [4,5,6]

(a) Concrete

(b) Steel rebars   (c) CFRP bars

Fig. 2 The material constitutive models for FEM analysis [8]

Structures [8]. The equations and compressive curve are listed in Fig. 2 (a). The Young's modulus of concrete had been found from the uniaxial concrete compression stress-strain relationship. The yield strength, was 1/3 of compressive strength, were found in the Standard Specifications for Concrete Structures, too. The plasticity for the concrete according to Drucker-Prager [7,11] was used.

(3) Steel rebars' parameter

The main steel rebars in the RC beams had been done in the laboratory [4,5,6]. The bi-linear strain-stress curve for steel rebars was used. After the yielding strength of the steel, the slope (tangent modulus) of 0.01Es would be used. Fig. 2 (b) shows the properties of steel. The Von Mises [7,11,12] yield surface for the steel rebars was used in this paper.

(4) CFRP bars' parameter

The main CFRP bars in the RC beams had been

done in the experiment [4, 5, 6)]. The strength of CFRP bars drops to zero when it reached to the tensile strength. Fig. 2 (c) shows the properties of steel rebars.

3.2 Analysis Procedure

The load steps were used for the non-linear analysis calculation. For the iteration processing, Quasi-Newton method [7)], using the information of previous solution vectors and out-of–balance force vectors during the increment to achieve a better approximation, was used with displacement and force norms for convergence criteria. Forty iterations would be used for each load steps, and convergence tolerance would be 0.001. The stop criterion for the FEM calculation was 0.006 that the concrete compressive strength reached.

4. Maximum Flexural Strength

The maximum flexural strength, deflection and failure condition are listed in Table 3. Fig. 3 shows the experimental and FEM results.

4.1 Experimental results

(1) N-C1S2

The RC beam N-C1S2 had the maximum flexural strength of 56.51 kN, and the deflection was 10.62 mm. The failure mode was bending failure. The cracks developed from the bottom of the RC beam and went up directly towards the loading area.

(2) N-C2S2

The RC beam N-C2S2 had the maximum flexural strength of 108.00 kN, and the deflection was 15.22 mm. The failure mode was bending failure. The cracks developed from the bottom of the RC beam and went up directly towards the loading area.

(3) N-C3S2

The RC beam N-C3S2 had the maximum flexural strength of 154.63 kN, and the deflection was 18.99 mm. The failure mode was bending failure. The cracks developed from the bottom of the RC beam and went up directly towards the loading area

4.2 FEM results

The assumption for the FEM RC beams failure was based on the uniaxial compression experimental results of maximum flexural strain. The location to be checked in the RC beams model is on the top center edge of the RC beams model under the loading area.

(1) N-C1S2

The RC beam N-C1S2 had the maximum flexural strength of 55.25 kN, and the deflection was 13.20 mm. Comparing the maximum flexural strength, the FEM

Table 3 Maximum flexural strength, deflection and failure modes

| Specimen | Maximum flexural strength (kN) | | Exp. | Deflection (mm) | | Failure |
	Experiment	FEM	FEM	Experiment	FEM	Condition
N-C1S2	56.51	55.25	1.02	10.62	13.20	Bending
N-C2S2	108.00	98.00	1.10	15.22	13.26	Bending
N-C3S2	154.63	118.00	1.31	18.99	12.20	Bending

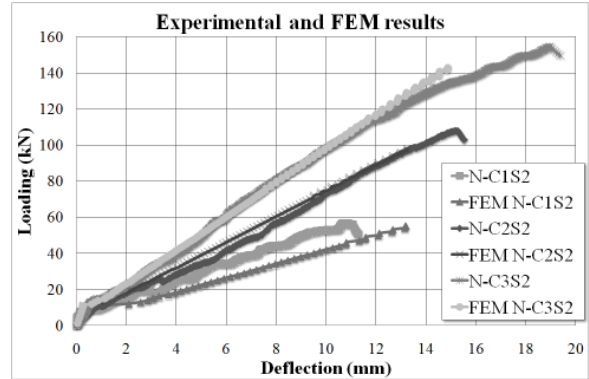

Fig. 3 Loading-Deflection relationships of RC beams with steel rebars and CFRP bar

result was approximately 2% less than the experimental results.

(2) N-C2S2

The RC beam N-C2S2 had the maximum flexural strength of 98.00 kN, and the deflection was 13.26 mm. Comparing the maximum flexural strength, the FEM result was approximately 10% less than the experimental results.

(3) N-C3S2

The RC beam N-C3S2 had the maximum flexural strength of 118.00 kN, and the deflection was 12.20 mm. Comparing the maximum flexural strength, the FEM result was approximately 31% less than the experimental results.

5. Strain of CFRP bars for the FEM Results

Fig. 4 shows the strain results of FEM for the steel rebars and CFRP bars. By using the experimental results, the yielding strain of the steel rebars had been checked and recorded from the FEM modeling results. Also, the tensile strain of the CFRP bars had been checked and recorded. The results can be found and calculated from Tables 2 and Table 3. The tensile stain of CFRP bar is 9.278332×10^{-3} ($= 854.72$ N/mm^2 / 92120 N/mm^2).

5.2 Loading-strain relationship of CFRP bars

As seen from Fig. 4, for N-C1S2, the result of FEM calculation for the CFRP tensile force was about
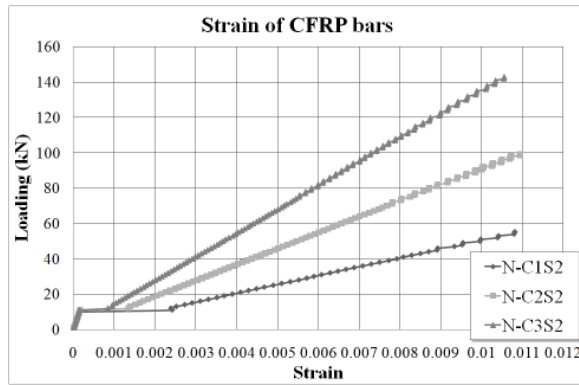
Fig. 4 Loading-Strain relationships of steel rebars and CFRP bars

46.00 kN. For N-C2S2, the result of FEM calculation for the CFRP tensile force was about 84.00 kN. For N-C3S2, the result of FEM calculation for the CFRP tensile force was about 126.00 kN. Moreover, as seen from Fig. 3 for the FEM results, the CFRP tensile force was reached before the failure of the RC beams that were 55.25 kN and 98.00 kN for N-C1S2 and N-C2S2, respectively. However, the CFRP tensile force was reached before the failure of the RC beams that was 118.00 kN for N-C3S2. From the behavior of rebars' strain, we can notice that the first cracks would happen around 10.00 kN, 11.00 kN, 11.00 kN for N-C1S2, N-C2S2, and N-C3S2, respectively. Finally, the FEM results of CFRP bars were similar to the experimental results also.

6. **Conclusion**

(1) For the RC beams with CFRP bars, the cracks developed from the bottom of the RC beam and went up directly towards the loading area. Moreover, all the RC beam specimens with the CFRP bars were bending failure.

(2) For the RC beams with one and two CFRP bars in the tensile side of the RC beams, the tensile strengths of CFRP bars were reached before the strain of the uniaxial compression strength. However, for the three CFRP bars in the tensile side of the RC beam, the tensile strain was reached after the strain of the uniaxil compression strength. This means that the RC beam with three CFRP bars still within the elastic region when the RC beams were assumed to fail in the FEM results.

(3) As seen from Fig. 3, the FEM results show that the FEM simulations have similar patterns to the experimental results. In other words, the FEM input parameters should be reconsidered again and

the interface between concrete and the steel rebars or FRP bars need to be included.

References:

1) Abdalla, H. A.: "Evaluation of Deflection in Concrete Members Reinforced with Fibre Reinforced Polymer (FRP) Bars," Composite Structures, Vol. 56, No. 1, pp. 63-71 (2002)

2) Toutanji, H. and Deng, Y.: "Deflection and Crack-Width Prediction of Concrete Beams Reinforced with Glass FRP Rods," Construction and Building Materials, Vol. 17, No. 1, pp. 69-74 (2003)

3) Wegian, F. M. and Abdalla, H. A.: "Shear Capacity of Concrete Beams Reinforced with Fiber Reinforced Polymers," Composite Structures, Vol. 71, No. 1, pp. 130-138 (2005)

4) Li, Y.-F., Lin, C.-T., Jau, W.-C., et al.: "A Feasibility Study on the Flexural RC Beams Using GFRP Rebars as the Main Reinforcement," Structural Engineering (Taiwan), Vol. 22, No. 4, pp. 113-128 (2007)

5) Li, Y.-F., Lin, C.-T., Hung, M.-J., et al.: "A Feasibility Study on Mechanics Behavior of the High Strength Concrete Beams with CFRP Bars," Structural Engineering (Taiwan), Vol. 24, No. 2, pp. 33-54 (2009)

6) Hsu, M.-C., Kida, T., Abe, T., et al.: "A Study on the Maximum Flexural Strength of RC Beams with Steel Rebars and CFRP Bars by Using FEM Analysis," JSCE 2009 Annual Meeting, V-564, pp. 1125-1126 (2009)

7) DIANA Finite Element Analysis User's Manual: TNO Building and Construction Research (2000)

8) Japan Society of Civil Engineers: Standard Specifications for Concrete Structures - 2002, Structural Performance Verification (2002)

9) Okamura, H., Maekawa, K.: Nonlinear Analysis and Constitutive Models of Reinforced Concrete, GIHODO printing, pp. 7~14 (1991)

10) Jan Gerrit Rots: Computational modeling of concrete fracture, PhD thesis, Delft University of Technology (1988)

11) Chen, W. F.: Plasticity in Reinforced Concrete, McGraw-Hill Book Company, pp. 83~85 (1982)

12) Jan G. M. van Mier: Fracture Processes of Concrete, CRC Press, Inc., Ch. 5 (1997)